MATHEMATICAL MODELLING AND DYNAMIC SIMULATION OF A PEM ELECTROLYSER

SUMMARY

This paper proposes a simple mathematical model of a PEM electrolyser. The dynamic simulation of the model is carried out, which allows the simulation of electrochemical, thermal and mass flow behaviours with enough precision for engineering applications. The model gives the operating voltage and outlet temperature from the input current and the inlet temperature conditions. The electrochemical submodel is validated using the previous literature. The results obtained from dynamic simulation is studied and the behaviour of different parameters like outlet temperature and voltage is observed. The results shows that there is corresponding change in outlet temperature with the current and voltage shows a slight different pattern at the point where the current changes due to overpotential. The variation due to change in stoichiometric is also analysed. The model is found to be consistent when compared with the literature.

Keywords: PEM Electrolyser, Mathematical Model, Dynamic Simulation, Overpotential.

1. INTRODUCTION

The population is going up daily. This population increase demands more and more goods and services that leads to increased necessity for energy supply [1]. Now fossil fuels are used to meet energy need, which is a problem maker, due to increase in concentration of carbondioxide in the atmosphere and leads to global warming. On another side petroleum is a small source for fuel that is decreasing rapidly and becoming more expensive. These fuels have less reserves, which is concentrated in certain region of the world [2].

In coming days hydrogen will be a sustainable source of energy carrier. Hydrogen can be used in fuel cells to generate electricity efficiently, with water as the only by-product. And also, hydrogen is the lightest element and any leakage of hydrogen gas can disperse quickly, thus hydrogen is also a safe energy source as other commonly used fuels [3]. It has a high energy yield of 122 kJ/g, which is 2.75 times greater than hydrocarbon fuels, it has good properties as a fuel for internal combustion engines in automobiles. Hydrogen can be used as a fuel directly in an internal combustion engine not much different from the engines used with gasoline. Hydrogen has very special properties as a transportation fuel, including a rapid burning speed, a high effective octane number, and no toxicity or ozone-forming potential. It has much wider limits of flammability in air (4-75% by volume) than methane (5.3-15% by volume) and gasoline (1-7.6% by volume) [2]. However, hydrogen is not an energy source, but an energy carrier. Hydrogen must be produced from other sources with energy input. Presently, hydrogen can be economically produced from hydrocarbon reforming, which is neither renewable nor clean from the life cycle point of view. Powered by solar energy, hydrogen can be produced from water, via photocatalysis, thermochemical cycles, and water electrolysis. These methods offer renewable and clean production of hydrogen fuel and, therefore, have attracted increasing research interests in recent years. So far, the efficiencies of photocatalysis and thermochemical cycles are still too low to be economically competitive. Water electrolysis is hence the most promising technology for large-scale hydrogen production [3].

Modelling of water electrolyser is a very useful tool for simulation and prediction of the behaviour of the systems of hydrogen generation. It will be very important when the electrolyser is coupled from a renewable source of electricity directly, since we can expect intermittent and variable supply. [4].

Here, a feasible electrolyser model was chosen by thorough study of different types of electrolyser and its characteristics were done. For our purpose we found that, compared with traditional alkaline electrolysis, in which corrosive potassium hydroxide (KOH) solution is used as the electrolyte, proton exchange membrane (PEM) electrolysis have more advantages, like ecological cleanness, high degree of gases purity, and easy maintenance. Because, the cost of hydrogen production by PEM electrolysis can be reduced further by continuous technology development, research on PEM electrolysis has become very active in recent years. Research and study on PEM electrolysis for hydrogen production are focused on demonstration of PEM electrolysis for hydrogen production, development of new catalysts, and development of new proton exchange membrane electrolytes [3].

There are numerous experimental studies that, investigates the PEM electrolysers in different aspects. However, modelling a PEM electrolyser is also necessary. Modelling a cell or stack has uttermost importance in understanding the operational behaviour of a PEM electrolyser. Many mathematical models/calculations exist for characterizing the cell component(s), using own code, employing statistical methods available software [5].

Since last few years, research interest has certainly increased around PEMWEs and specific PEMWE models. Choi et al. [6] developed a simple model based on Butler-Volmer kinetics but only covering the electrochemical behaviour. Görgün described a complete dynamic model based on conservation of molar balance at the anode and the cathode [7], but it has not been experimentally validated. Certain researchers of the University of North Dakota (USA) modelled the polarization performance of a 6kW PEMWE by developing a semi-empirical equation [8 - 10]. The basics of equation is thermodynamic principles and Butler-Volmer kinetics. From the results of experiment they also analysed the effect of the temperature in the exchange current densities at the electrodes, the PEM conductivity and the anode transfer coefficient. At the latest, Marangio et al. [11, 12] presented a complete model validated on a high pressure PEMWE. Their work takes into account the concentration overpotential, the mass flows inside the electrolytic cells and makes a complex modelling of the ohmic losses in electrodes and plates and in the membrane. The work of Lebbal et al. [13] also takes into account the concentration overpotential that model the kinetics of the reaction and propose a non-linear square identification method to estimate the parameters of the model. Even though the dependency of temperature is not clear enough, this approach is quite interesting regarding the used identification and monitoring methods [4].

Almost all the modelling studies are mainly focused on the physics or the behaviour of a cell or a stack. The behaviour of a PEM electrolyser depending on the operating conditions should be investigated when designing a system. Above all, building a system using the optimized parameters of a cell/ stack is also quite important. Sometimes, the operating parameters of the cell or stack may subject to change according to the other system components properties. Also, the properties of other components such as power supply, water pump, water tank, cooling system, control unit, etc. should also be considered when deciding system components and the range of operating parameters. Literature has various system modelling studies regarding fuel cells. However, a study dedicated to system modelling including a PEM electrolyser is less and as far as researcher's knowledge. Dale et al. [14] modelled a commercial PEM electrolyser cell in a system containing balance of plant, but it didn't include the system components to the model. This type of system should continuously decided on the operating conditions according to environmental conditions and previous operating conditions when it is running [5].

Yalcinoz et al. [15] dynamically modelled an air breathing PEM fuel cell with a feedback control system. Gorgun et al. [16] gives a dynamic model of PEM electrolyser unit. The model is based on mole balance equations at anode and cathode. The partial pressure calculation of liquid water at anode side is done based on ideal gas equation. However, a comparative study with experimental data has been made to validate the model. Dale et al. [17] developed a semi-empirical model of PEM electrolyser system considering temperature dependent reversible cell voltage. Curve fitting methods are used to fit the experimental data to determine various model parameters. Biaku et al. [18] made the study of temperature dependence of charge transfer coefficient at the anode by a semi-empirical model. Santarelli et al. [19] analysation was on the effects of temperature, pressure and water feed rate on the electrolyser operation with the help of a regression model. In another work, Marangio et al. [20] presented a theoretical model of electrolyser system in detail. The presented model includes activation, ohmic and diffusion overvoltages. It takes into account the resistances of electrodes and plates and also resistance of membrane. The model is fitted to experimental data and a detailed analysis of operating parameters on electrolyser performance is presented, even though, the models discussed above are semi-empirical in nature. In an investigation a model is developed based on analytical expressions, which is dynamically an electrolyser system under a wide range of operating conditions, e.g., temperature and pressure [21].

This paper focusses on hydrogen production using a dynamic electrolyser. The electrolyser is modelled using the energy balance principle. At first the electrochemical equations are formed and the behaviour is validated. Then, the mass concentrations at the inlet and outlet, the heat generated and the thermal energy terms are equated and a differential equation is obtained. This differential equation is solved and matlab simulation is done.

2. PRINCIPLE OF OPERATION

Electrolysis is one of the good option for hydrogen production from renewable resources. Electrolysis is the process of splitting water into hydrogen and oxygen using electricity. This reaction takes place in a unit called an electrolyser. Size of electrolysers can range from small, appliance-size equipment that is well-suited for small-scale hydrogen production to large-scale, central production system that could be attached directly to renewable or other non-greenhouse-gas-emitting sources of electricity [22].

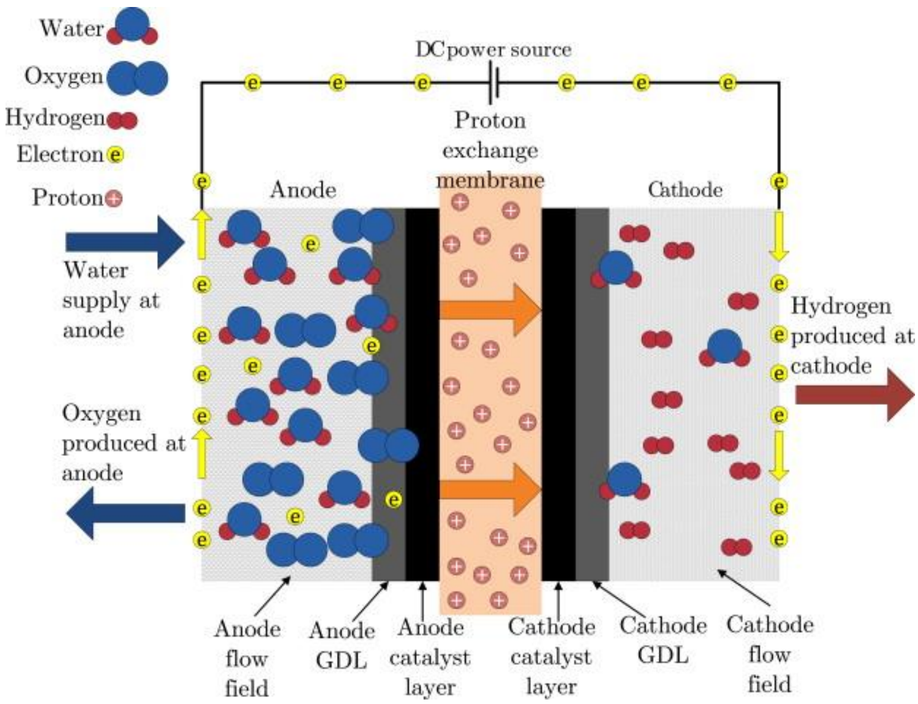

Figure 2.1: Schematic diagram of an Electrolyser [23]

- Water reacts at the anode to form oxygen and positively charged hydrogen ions (protons).
- The electrons flow through an external circuit and the hydrogen ions selectively move across the PEM to the cathode.
- At the cathode, hydrogen ions combine with electrons from the external circuit to form hydrogen gas.

Anode: $H_2O \longrightarrow 2H^+ + 1/2O_2 + 2e^-$ 2.1

Cathode: $2H^+ + 2e^- \longrightarrow H_2$ 2.2

Total: $H_2O \longrightarrow H_2 + 1/2O_2$ 2.3

2.1. Thermodynamics

Thermodynamic calculation provides functional relations of reversible voltage, thermoneutral voltage and change in Gibbs free energy with temperature. To calculate the thermodynamic effects in electrolytic reaction, it is convenient to assume hydrogen and oxygen gases partial pressure are equal to water pressure, which is operated at atmospheric pressure [24].

Reaction enthalpy:

$$\Delta H(T, P_i) = \Delta H_{H_2} + \frac{1}{2}\Delta H_{O_2} - \Delta H_{H_2O} \qquad 2.4$$

P_i= partial pressure of species i (i=H_2O,H_2, O_2)

At standard conditions ($T^0 = 298K,\ P^0 = 10^5 Pa$)

$$\Delta H^0_{liq} = -285.8kJ/mol_{H_2},$$

$$\Delta H^0_{vap} = -241.8kJ/mol_{H_2}$$

Reference Potential E_{ref}

$$E_{ref}(\mathrm{T}, P_i) = -\frac{\Delta H(T,P_i)}{2F} \qquad 2.5$$

F = Faraday's constant (F= 96485$Cmol^{-1}$)

$$E^0_{ref,liq} = 1.48V$$

$$E^0_{ref,vap} = 1.25V$$

Reaction entropy:

$$\Delta S(T, P_i) = \Delta S_{H_2} + \frac{1}{2}\Delta S_{O_2} - \Delta S_{H_2O} \qquad 2.6$$

Standard (for liquid water) and saturated (for vapour)

$$\Delta S^0_{liq} = -163.3\, JK^{-1}mol^{-1}_{H_2}$$

$$\Delta S^0_{liq}(T^0, P_{sat}(T^0)) = -16\, JK^{-1}mol^{-1}_{H_2}$$

The entropy variation generates a heat production that can be expressed by [25]:

$$Q = T\Delta S \qquad 2.7$$

Electrical energy available for the user in ideal conditions is given by the variation of the Gibbs free energy that is defined by:

$$\Delta G(T,P_i) = \Delta H(T,P_i) - T\Delta S(T,P_i) \quad 2.8$$

Reversible electrical work:

$$W_{elec}^{rev} = -\Delta G \quad 2.9$$

In standard conditions:

$$\Delta G^0 = -237.1 kJ/mol_{H_2}$$

Enthalpy can be obtained by:

$$\Delta\widehat{h_f} = \Delta\widehat{h_f^0} + \int_{T_0}^{T} C_p(T)dT \quad 2.10.a$$

Integrating,

$$\Delta\widehat{h_f} = \Delta\widehat{h_f^0} + C_p(T)(T - T_0) \quad 2.10.b$$

For the electrolysis reaction the total enthalpy can be formulated as:

$$\Delta H(T,P_i) = \Delta H_{H_2} + \frac{1}{2}\Delta H_{O_2} - \Delta H_{H_2O} \quad 2.10.c$$

Entropy can be obtained by:

$$\hat{s} = \widehat{s^0} + \int_{T_0}^{T} \frac{C_p(T)}{T} dT \quad 2.11.a$$

Integrating,

$$\hat{s} = \widehat{s^0} + C_p(T) ln\left(\frac{T}{T_0}\right) \quad 2.11.b$$

For the electrolysis reaction the total entropy can be formulated as:

$$\Delta S(T,P_i) = \Delta S_{H_2} + \frac{1}{2}\Delta S_{O_2} - \Delta S_{H_2O} \quad 2.11.c$$

Ideal Cell voltage:

$$E_{rev}(T,P_i) = \frac{\Delta G(T,P_i)}{2F} \quad 2.12$$

E_{rev} is also called as the reversible open circuit voltage (OCV). In standard conditions,

$$E_{rev}^0 = \frac{\Delta G^0}{2F} = 1.23\ V$$

Assuming that hydrogen, oxygen and vapour behave like ideal gases, $\Delta G(T, P_i)$ [25]:

$$\Delta G(T, P_i) = \Delta G^0 - \int_{298K}^{T} \Delta S(T, P^0) dT + RT \ln\left(\frac{a_{H_2} a_{O_2}^{\frac{1}{2}}}{a_{H_2O}}\right) \quad 2.13$$

$$a_i = (activity\ of\ species\ i) = P_i/P^0$$

$$E_{rev}(T, P_i) = 1.229 - 85.10^{-5}(T - 298) + \frac{RT}{2F} \ln(a_{H_2} a_{O_2}^{\frac{1}{2}}) \quad 2.14$$

$$E_{rev}(T, P_i) = 1.184 - 23.10^{-5}(T - 298) + \frac{RT}{2F} \ln\left(\frac{a_{H_2} a_{O_2}^{\frac{1}{2}}}{a_{H_2O}}\right) \quad 2.15$$

$$E_{rev}(T, P_i) = E_{th}(T, P^0) + \frac{RT}{2F} \quad 2.16$$

3. ELECTROCHEMICAL SUBMODEL

A feature that distinguishes the electrochemical reactions is its ability to manipulate the size of the activation barrier by varying the cell potential. Charged species are involved as either reactants or products in all electrochemical reactions. The free energy obtained from charged species is its sensitivity to voltage. Therefore, changing the cell voltage changes the free energy of the charged species taking part in a reaction, thus affecting the size of the activation barrier [4].

The performance of electrolysis cells are typically compared by plotting their polarization curves, which is obtained by plotting the cell voltage against the current density. The main sources of increased voltage in a PEM electrolyser are ohmic losses, activation losses and concentration losses, which is explained in the coming sections [26].

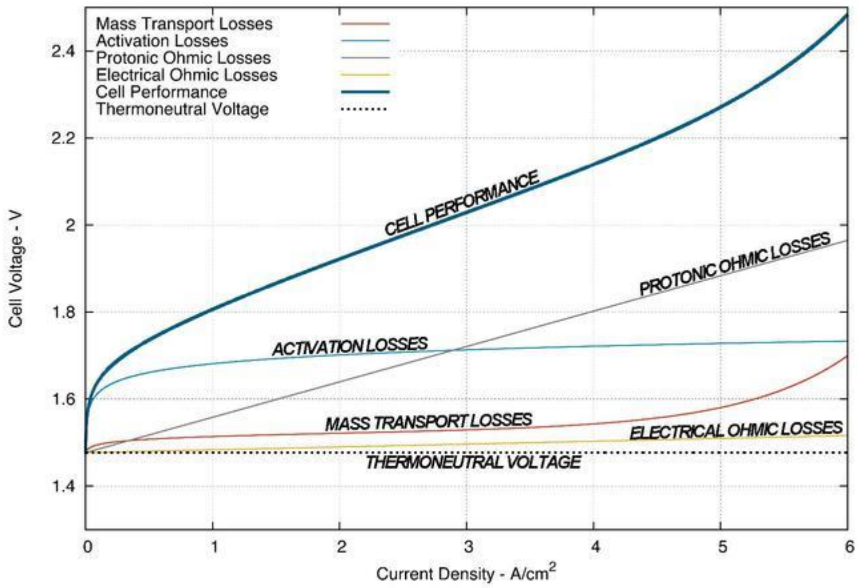

Figure 3.1: Polarization curve depicting the various losses attributed to PEM electrolysis cell operation [26]

Cell voltage:

$$V_{cell} = U_{rev} + \eta_{act} + \eta_{ohmic} + \eta_{conc} \quad 3.1$$

3.1. Reversible Potential

The open circuit voltage or reversible potential of the cell (U_{rev}) can be derived from the Nernst equation of water electrolysis. Nernst potential for water electrolysis at constant atmospheric pressure is empirically given as:

$$U_{rev}(T) = 1.5184 - 1.5421 * 10^{-3}T + 9.523 * 10^{-5}T\ lnT + 9.48 * 10^{-8}T^2 \quad 3.2.a$$

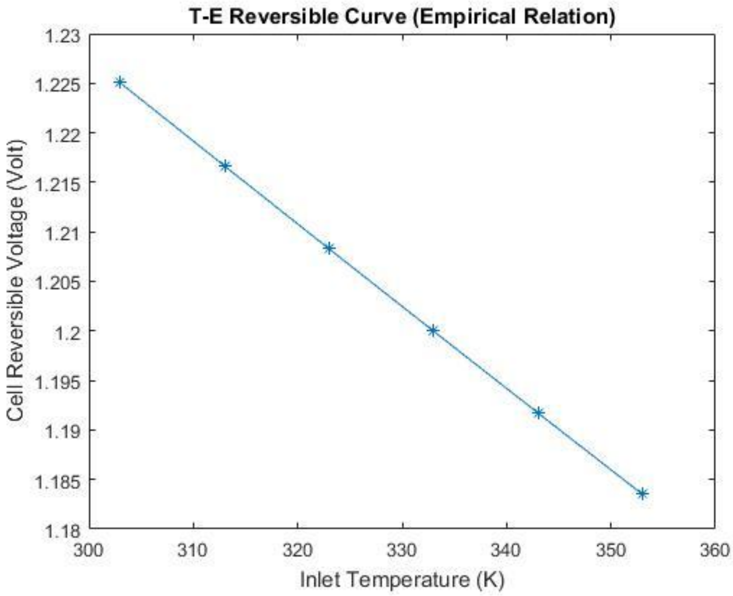

Figure 3.2: Inlet Temperature vs Cell Reversible Voltage (Using Equation 18.a)

Figure 3.2, shows the variation of reversible voltage with the inlet temperature and it is observed that the reversible voltage is decreasing as the temperature increases.

Nernst potential for water electrolysis for pressure variation:

$$U_{rev}(T,P) = E^0(T,P) + \frac{RT}{2F}\ln\left(\frac{P_{H_2}P_{O_2}^{\frac{1}{2}}}{a_{H_2O}}\right) \quad 3.2.b$$

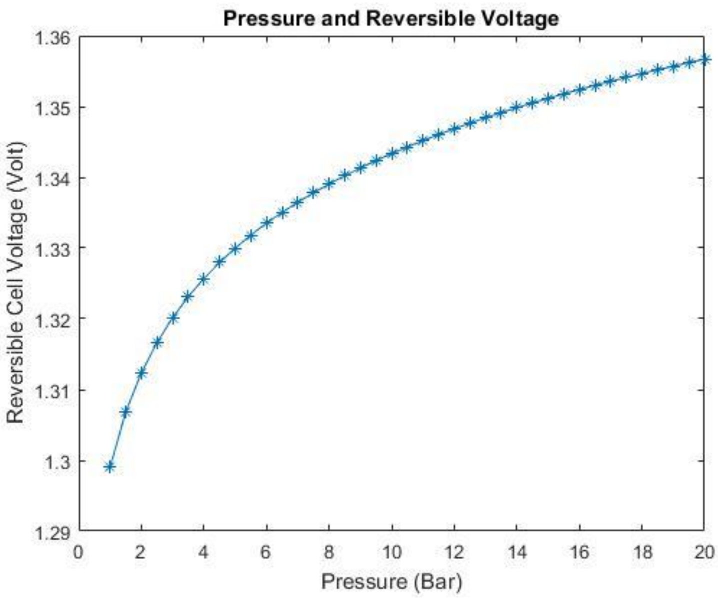

Figure 3.3: Pressure vs Cell Reversible Voltage (Using Equation 18.b)

Here we assume isobaric condition. At Standard Temperature = 298K

From Figure 3.3, it is observed that there is an increase in reversible cell voltage while using the equation 3.3. Hence we can conclude that there is an influence of pressure in reversible cell voltage at constant temperature.

3.2. Overpotentials

Overpotential is the potential difference (voltage) between a half-reaction's thermodynamically determined reduction potential and the potential at which the redox event is experimentally observed. In an electrolytic cell the existence of overpotential implies the cell requires more energy than thermodynamically expected to drive a reaction [27].

3.2.1. Activation Overpotential

When current flows through the electrolysis cell, charge transfer and mass-transport phenomena at the electrodes must be considered. These limitations of the semi reactions are known as activation and diffusion overpotentials.

Initially assuming only charge transfer limitations (accurate approximation only for low current densities) the Butler-Volmer expression relates the current density to the activation overpotential at each electrode [28-29]:

The general form:

$$i = i_0 \left\{\frac{R^o}{R^*}\exp\left(\beta\frac{ZF\eta_{act}}{RT}\right) - \exp\left[-\left(\frac{O^o}{O^*}\right)(1-\beta)\frac{ZF\eta_{act}}{RT}\right]\right\} \qquad 3.3.a$$

$R^*, O^* = Concentration\ when\ i = 0$

$R^o, O^o = Concentraion\ when\ i \neq 0$

Considering the ratio of concentrations at i = 0 and i ≠ 0 as 1, we can write above equation as,

$$i = i_0 \left\{\exp\left(\beta\frac{ZF\eta_{act}}{RT}\right) - \exp\left[-(1-\beta)\frac{ZF\eta_{act}}{RT}\right]\right\} \qquad 3.3.b$$

Where,

$i = actual\ current\ density\ in\ the\ electrolyser$

$i_0 = exchange\ current\ density$

$\eta_{act} = activation\ polarization$

$F = Faraday's\ constant = 96485\ Cmol^{-1}$

$R = Gas\ constant = 8.314\ 4621\ \mathrm{J}K^{-1}mol^{-1}$

$\beta = Symmetry\ factor\ for\ the\ electrode$. It represents physically the fraction of additional energy that goes towards the reduction (β) and to the oxidation$(1-\beta)$.

$Z = stoichiometric\ coefficient\ for\ transferred\ electrons = 2,$
$for\ water\ electrolysis.$

Also reduction $(\beta) = \ \alpha_R$ and oxidation$(1-\beta) = \alpha_O$

Hence we write equation 19.b as,

$$i = \ i_0 \left\{\exp\left(\alpha_R \frac{ZF\eta_{act}}{RT}\right) - \exp\left[\alpha_O \frac{ZF\eta_{act}}{RT}\right]\right\} \qquad 3.3.c$$

For low activation polarization,

We know,

$$e^x = 1 + x + \frac{x^2}{2!} + \frac{x^3}{3!} + \cdots \qquad 3.4$$

Neglecting higher terms and substituting equation (18) in (17), we get

$$i = \ i_0 \frac{(\alpha_R + \alpha_O)ZF}{RT}\eta_{act} \qquad 3.5$$

But we know take, $\alpha_R + \alpha_O = 1$.

Hence we can take for low activation potential,

$$\eta_{act} = \ \frac{2RT}{ZF}\ \frac{i}{i_0}\ \text{, when } \beta = 0.5. \qquad 3.6$$

For high activation polarization,

$$\eta_{act} = \frac{2RT}{ZF}\ ln\left(\frac{i}{i_0}\right)\text{, when } \beta = 0.5. \qquad 3.7$$

This is known as Tafel equation.

Therefore, anodic (η_a) and cathodic (η_c) activation overpotential:

$$\eta_a = \frac{RT}{\alpha_a ZF}\ ln\left(\frac{i_a}{i_{0,a}}\right) \qquad 3.8$$

$$\eta_c = \frac{RT}{\alpha_c ZF}\ ln\left(\frac{i_c}{i_{0,c}}\right) \qquad 3.9$$

Temperature dependence of i_0 can be modelled using Arrhenius form as,

$$i_0 = i_{0,ref}\, exp\left[-\frac{E_{exc}}{R}\left(\frac{1}{T}-\frac{1}{T_{ref}}\right)\right] \qquad 3.10$$

Where, $E_{exc} = activation\ energy\ for\ the\ electrode\ reaction,$

$i.e., activation\ energy\ of\ the$" water oxidation" $for\ the\ anode\ electrocatalyst$

The exchange current density for Pt-Ir anode = 10^{-7} A/cm^2 and Pt cathode = 10^{-3} A/cm^2 at 80^0C (for reference value).

3.2.2. Concentration Overpotential

The diffusion or concentration overpotential (η_{conc}) can be modelled by adding a limiting current term ($i_{L,a}$) to the anodic overpotential. The limiting current is the limiting value of a faradaic current that is approached as the rate of charge-transfer to an electrode is increased, i.e, as reaction proceeds faster, at some point all the reactant that reaches the electrode get consumed immediately. At this point ion concentration is zero, and the current levels off [30-31].

We consider concentration overpotential for very high current density. The anodic contribution is dominant because the oxygen bubbles would block the electrodic surface due to their larger volume [24, 25, 4].

$$\eta_{conc} = \frac{RT}{\alpha_a ZF}\, ln\left(\frac{i_L}{i_L - i_a}\right) \qquad 3.11$$

3.2.3. Ohmic Losses

Overpotential due to ohmic losses (η_{ohmic}) is another important effect. The dominant losses in η_{ohmic} are the ionic losses caused by the resistance to the proton transport through the PEM.

$$R_{ohmic} = R_{ion} + R_{ele} \qquad 3.12$$

$R_{ohmic} = ohmic\ resistance$

$R_{ion} =$ Ionic resistance

$R_{ele} = electronic\ resistance$

i.e, ohmic resistance consists of Ionic resistance and electronic resistance.

$$R_{ion} = \frac{t_m}{\sigma} \qquad 3.13$$

Where, $t_m = thickness\ of\ the\ membrane$

$\sigma = conductivity\ of\ the\ membrane.$

Using Arrhenius expression we can model the temperature dependence of the membrane conductivity.

$$\sigma(T) = \sigma_{ref}\ exp\left[-\frac{E_{pro}}{R}\left(\frac{1}{T} - \frac{1}{T_{ref}}\right)\right] \qquad 3.14$$

Where, $E_{pro} = temperature - independent\ parameter,$

$which\ represents\ the\ activation\ energy\ for\ proton\ transport\ in\ the\ membrane.$

Assuming membrane fully hydrated.

Here we consider $R_{ele} \ll R_{ion}$

Hence, $\eta_{ohmic} = R_{ohmic} * i$ 3.15

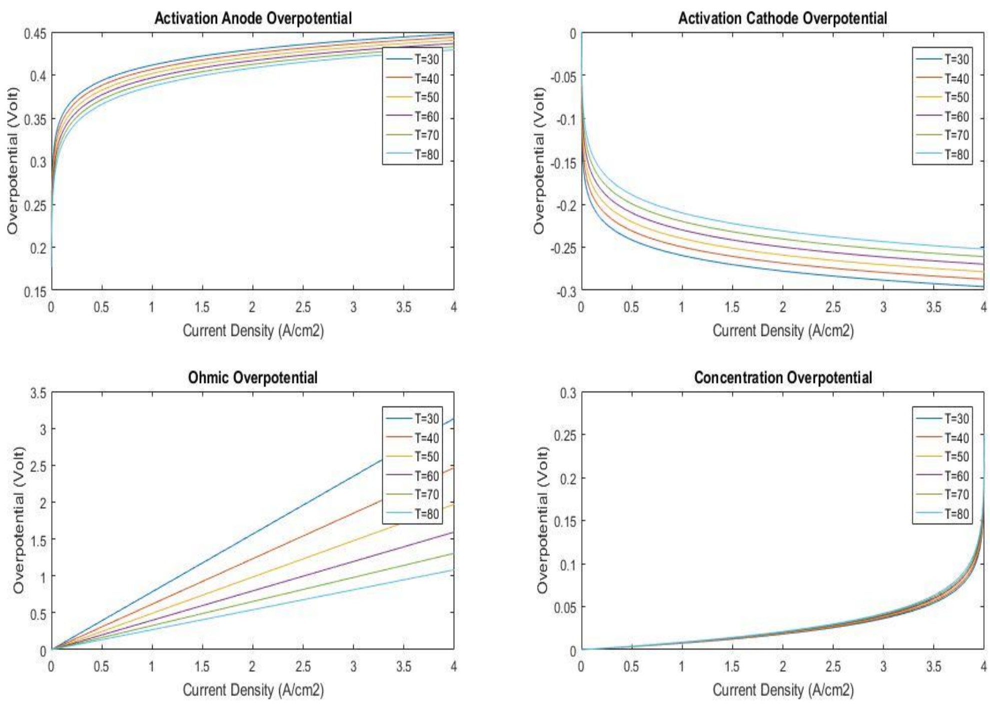

Figure 3.4: Overpotential Curves: (i) Activation Anode Overpotetential (ii) Activation Cathode Overpotetential (iii) Ohmic Overpotetential (iv) Concentration Overpotetential

The above figure gives the behaviour of different overpotentials. It is noted that there is gradual increase in the activation anode overpotential and gradual decrease in activation cathode overpotential. For concentration overpotential there is slight increase. For ohmic overpotential there is a linear increase and it gives much higher values compared to others. Hence we can say that ohmic overpotential is the most significant parameter in the overpotentials.

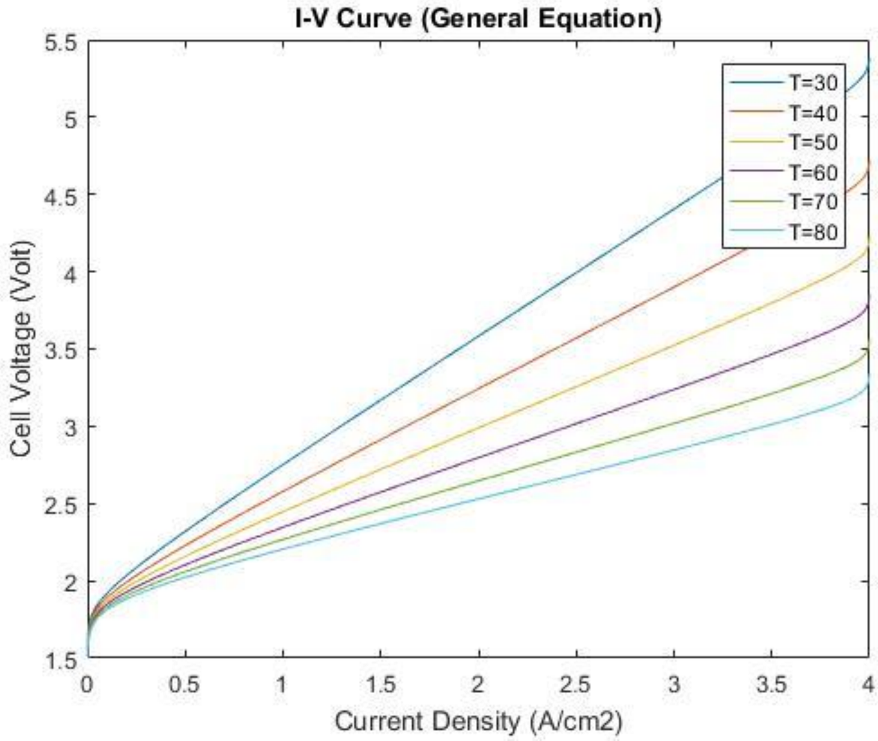

Figure 3.5: Polarization Curve

Figure 3.4, shows the polarization curve, which is a relation between current density and cell voltage. It is observed that there is gradual increase in voltage as the current density increases. It is also noticed that the lower inlet temperature gives higher cell voltage as compared to the higher inlet temperature. This can be justified by using figure 3.3, i.e, as the inlet temperature is lower there is high overpotential loss. By considering this we can say that, polarization curve shows lower values for higher inlet temperature.

3.3. Hydrogen production submodel

The molar flow rates of hydrogen and oxygen production and consumed water can be given using Faraday's law [4]:

$$M_{H_2}\left(\frac{mol}{s}\right) = \frac{I}{2F} * S_{cell} * \eta_F \tag{3.16}$$

$$M_{O_2}\left(\frac{mol}{s}\right) = \frac{I}{4F} * S_{cell} * \eta_F \tag{3.17}$$

$$M_{H_2O}\left(\frac{mol}{s}\right) = \frac{I}{2F} * S_{cell} * \eta_F \tag{3.18}$$

Where,

$I = current\ across\ the\ cell\ electrodes$

$S_{cell} = S_{single\ cell} * number\ of\ cells$

$\eta_F = Faraday's\ efficiency$, generally assumed to be more than 99%

The simulation of the proposed model is done and validated. It can be concluded that the model is good and shows similar graphical pattern when compared with the results of "Simple PEM water electrolyser model and experimental validation" [4].

4. DYNAMIC MODEL OF ELECTROLYSER

Incorporating the phenomenological relationships obtained from the last section a dynamic system of a PEM electrolyser is modelled. The unsteady components of mass and energy balance equations are considered. In this model, the fluid flow description is simplified by assuming that the water and gas flow simultaneously at the same speed, constant pressure in each fluid channel, a fully hydrated membrane and no dynamics for electrochemical phenomena that are orders of magnitude faster than other phenomena [32].

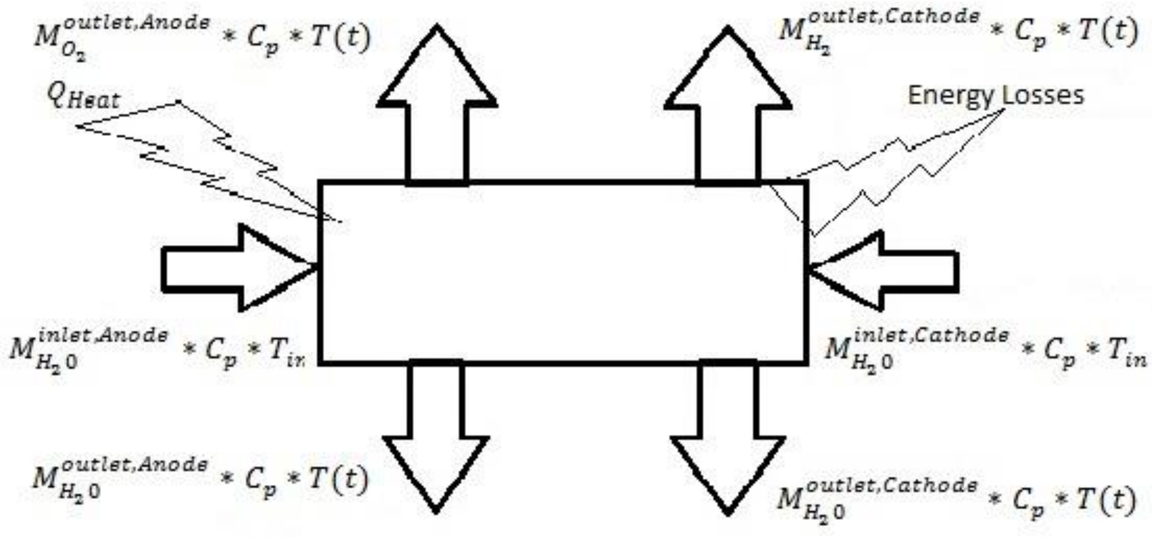

Figure 4.1: Energy Balance Schematic Diagram

Here,

$M_{H_20} = Mass\ concentration\ of\ water,$

$M_{H_2} = Mass\ concentration\ of\ Hydrogen,$

$M_{O_2} = Mass\ concentration\ of\ Oxygen,$

$C_{p_{H_20}} = specific\ Heat\ of\ water,$

$T_{in} = Inlet\ Temperature,$

$T(t) = Outlet\ Temperature\ varying\ with\ Time,$

$T = Average\ Outlet\ Temperature = (T_{in} +\ T(t))/2.$

Table 4.1: The constant and reference values

Sl. No	Parameter	Value	Reference
1	F (Faraday Constant)	96485 C/mol	Constant
2	R (Universal Gas Constant)	8.314 J/mol.K	Constant
3	il (Limiting Current)	4 A/cm^2	4
4	i0a (Current Density at Anode)	10^-7 A/cm^2	4
5	i0c (Current Density at Cathode)	10^-3 A/cm^2	4
6	Alpha (Charge Transfer Coefficient)	0.5	4
7	Eexc (Activation Energy for Electrode Reaction)	53990.065 J/mol	4
8	sigma_ref (Reference Conductivity of Membrane)	0.020 S/cm	
9	Epro (Activation Energy for Proton Transport in Membrane)	18912.42 J/mol	4
10	delta (Thickness of membrane,)	7*2.54*10^-3 cm	

4.1. Unsteady-state balance equation

Mass Concentration:

The mass balances of the liquid and gas phase water in the anode and cathode channels can be written as follows:

Inlet

$$M_{H_20}^{inlet,Anode} = (1 + \lambda_{Anode})\frac{I}{2F} * s * (18 * 10^{-3})\ (\frac{Kg}{S}) \qquad 4.1$$

$$M_{H_20}^{inlet,Cathode} = \lambda_{Cathode} * \frac{I}{2F} * s * (18 * 10^{-3})\ (\frac{Kg}{S}) \qquad 4.2$$

$Where, \lambda = Stoichiometric\ value.$

$$Voltage = \left(V(I) - \frac{\Delta H}{2F}\right) * I * s\ (Watt) \qquad 4.3$$

From equation (17),

$$V(I) = E_{rev}(T, P_i) + \eta_a - \eta_c + \eta_{conc} + \eta_{ohmic}$$

From equation (10.c),

$$\Delta H = \Delta H_{H_2} + \frac{1}{2}\Delta H_{O_2} - \Delta H_{H_2O}$$

<u>Outlet</u>

$$M_{H_20}^{outlet,Anode} = \lambda_{Anode} * \frac{I}{2F} * s * (18 * 10^{-3})\ (\frac{Kg}{S}) \qquad 4.4$$

$$M_{H_20}^{outlet,Cathode} = \lambda_{Cathode} * \frac{I}{2F} * s * (18 * 10^{-3})\ (\frac{Kg}{S}) \qquad 4.5$$

The mass balances of the hydrogen in the anode and cathode channels can be written as follows:

$$M_{H_2}^{outlet,Anode} = \frac{I}{2F} * s * (2 * 10^{-3})\ (\frac{Kg}{S})\ , (Negligable, assuming\ no\ crossover)$$

4.6

$$M_{H_2}^{outlet,Cathode} = \frac{I}{2F} * s * (2 * 10^{-3})\ (\frac{Kg}{S}) \qquad 4.7$$

The mass balances of the oxygen in the cathode channel can be written as follows:

$$M_{O_2}^{outlet,Anode} = \frac{I}{4F} * s * (32 * 10^{-3})\ (\frac{Kg}{S}) \qquad 4.8$$

Energy Balance:

The energy balance terms involving mass in, mass out, heat generation and total thermal energy of the cell through the MEA.

$$\rho C_p V \frac{dT}{dt} = \left[M_{H_20}^{inlet,Anode} * C_{p_{H_20}} * T_{in}\right] + \left[M_{H_20}^{inlet,Cathode} * C_{p_{H_20}} * T_{in}\right] + \left[\left(V(I) - \frac{\Delta H}{2F}\right) * I(t) * s\right] - [M_{H_20}^{outlet,Anode} * C_{p_{H_20}} * T(t)] - [M_{H_20}^{outlet,Cathode} * C_{p_{H_20}} * T(t)] - [M_{H_2}^{outlet,Cathode} * C_{p_{H_20}} * T(t)] - [M_{O_2}^{outlet,Anode} * C_{p_{H_20}} * T(t)]$$

4.9

$$\underbrace{\rho C_p V}_{Z}\frac{dT}{dt} = \underbrace{\left\{M_{H_20}^{inlet,Anode} * C_{pH_20} + M_{H_20}^{inlet,Cathode} * C_{pH_20}\right\}}_{X_{inlet}} T_{in} + \underbrace{\left[\left(V(I) - \frac{\Delta H}{2F}\right) * I(T,t) * s\right]}_{Q_{Heat}} -$$

$$\underbrace{\left\{M_{H_20}^{outlet,Anode} * C_{pH_20} + M_{H_20}^{outlet,Cathode} * C_{pH_20} + M_{H_2}^{outlet,Cathode} * C_{pH_20} + M_{O_2}^{outlet,Anode} * C_{pH_20}\right\}}_{Y_{outlet}} \mathrm{T(t)}$$

4.10.a

$$Z\frac{dT}{dt} = X_{inlet}T_{in} + Q_{Heat} - Y_{outlet}T(t) \qquad 4.10.b$$

The above differential equation is solved using an implicit method. By solving this differential equation the output temperature is obtained for transient conditions, for different inlet temperatures and stoichiometric values. The relations obtained are simulated in matlab.

5. RESULTS AND DISCUSSION

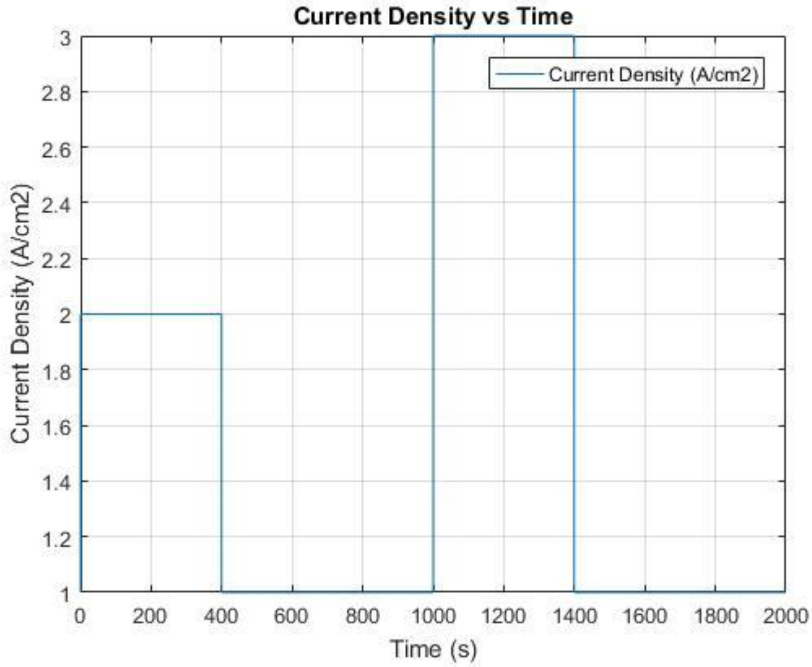

Figure 5.1: Current Density (Step Current) vs Time

The step current is shown in figure 5.1. At first there is a step from 1A/cm^2 to 2 A/cm^2, and then there is another step introduced at 1000s from 1 A/cm^2 to 3 A/cm^2.

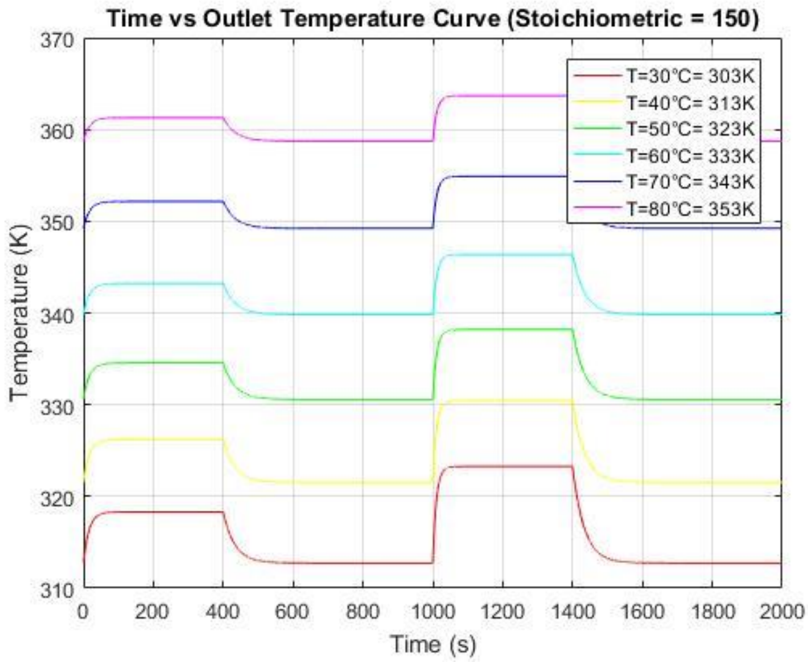

Figure 5.2: Time vs Outlet Temperature (For Different Inlet Temperatures)

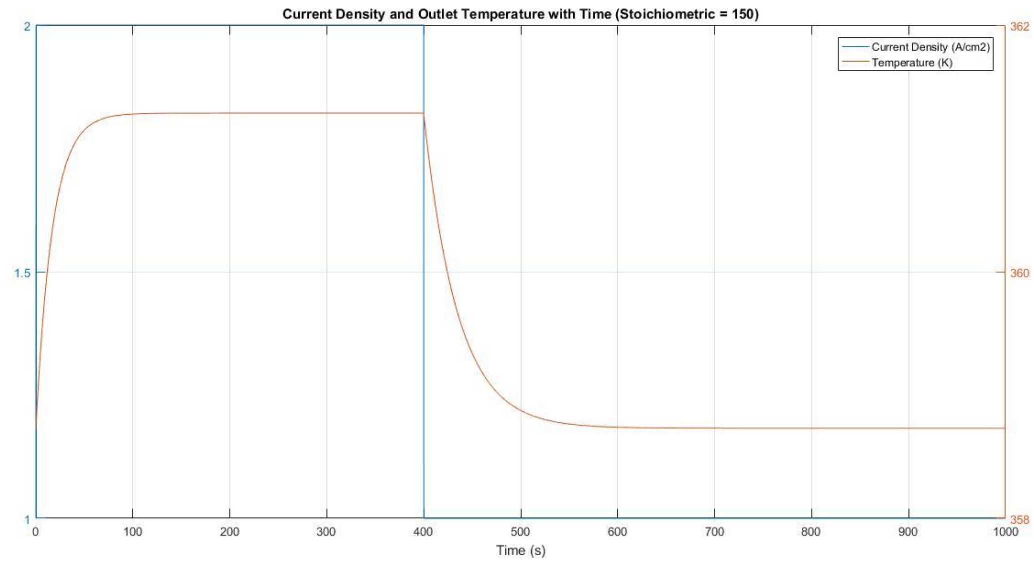

Figure 5.3: Current Density and Outlet Temperature with Time

From the figure 5.2 & 5.3, it is observed that the temperature various with current. As the current increases the temperature also increases gradually and as the current decreases the temperature also decreases gradually and remain constant. In figure 5.3, it is clearly observed that there is time lag for temperature to reach its exact outlet temperature when the current increases and also a time lag when the current decreases.

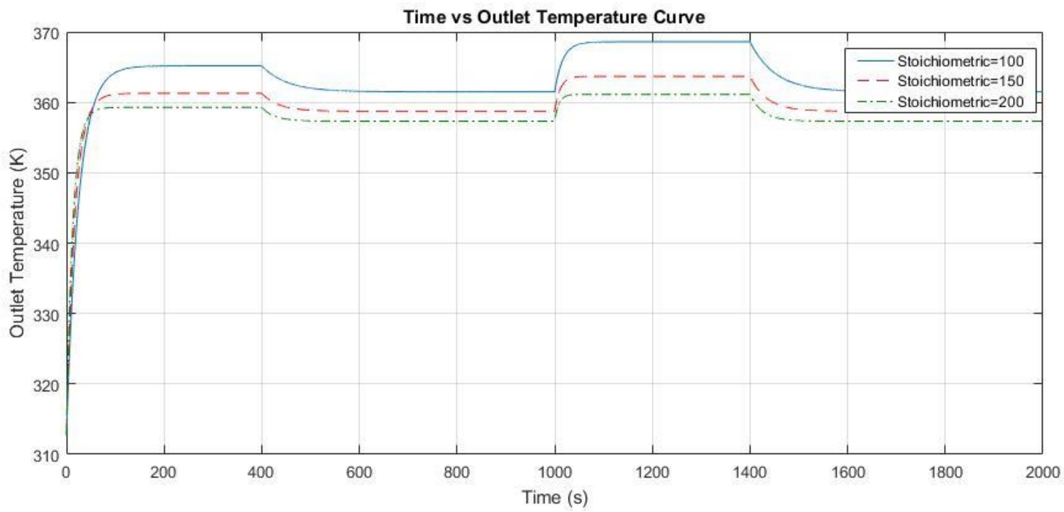

Figure 5.4: Time vs Outlet Temperature (for different stoichiometric)

From figure 5.4, it is observed that the outlet temperature increases as the stoichiometry decreases for same inlet temperature. For electrolyser the stoichiometric value is taken to be higher. This help to maintain the temperature of the electrolyser without any external means. Here, it can be clearly seen that the outlet temperature is decreasing with the increasing stoichiometric value and so we can say that there is a cooling effect.

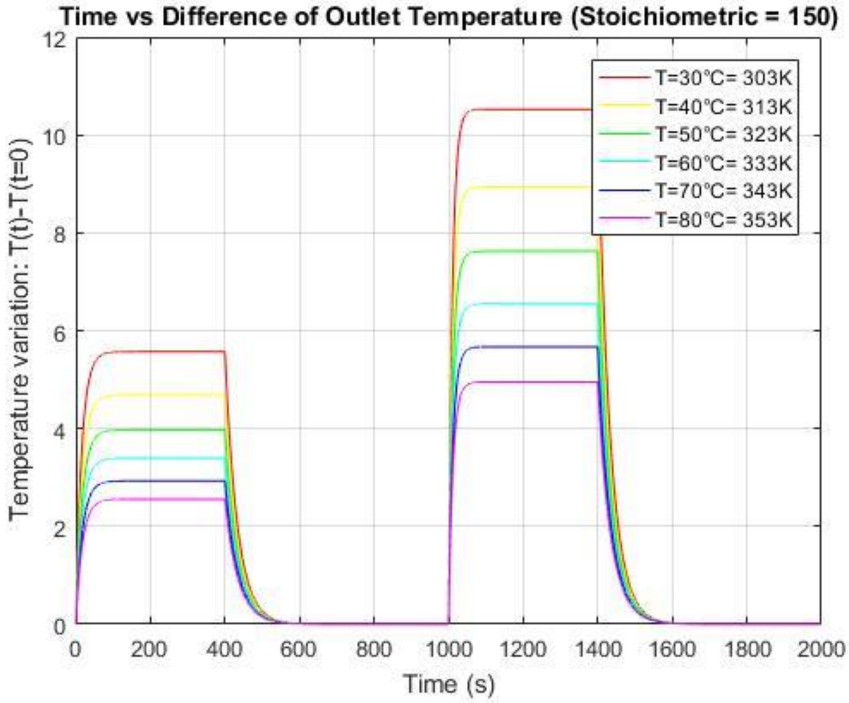

(a)

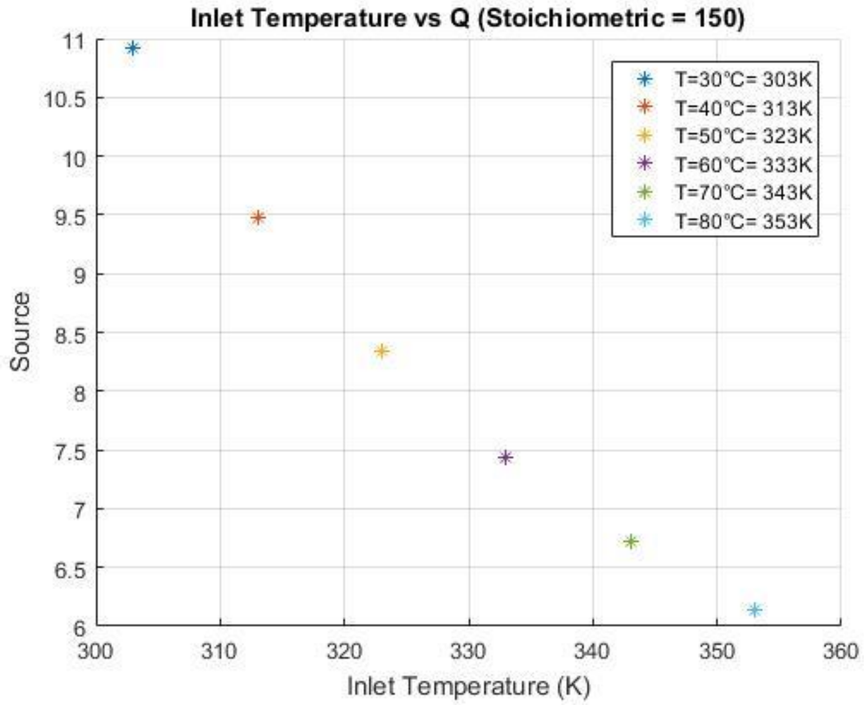

(b)

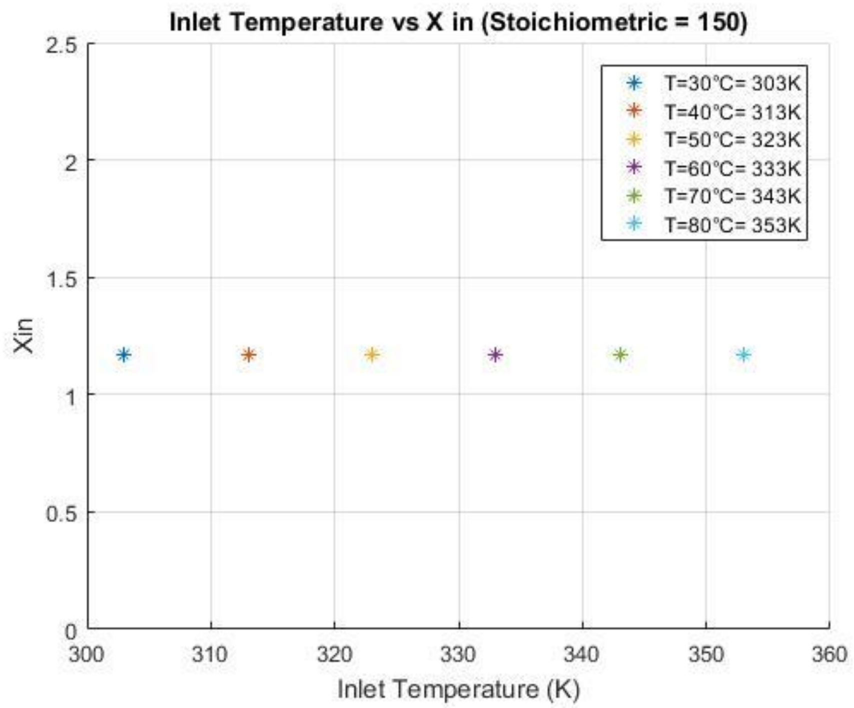

(c)

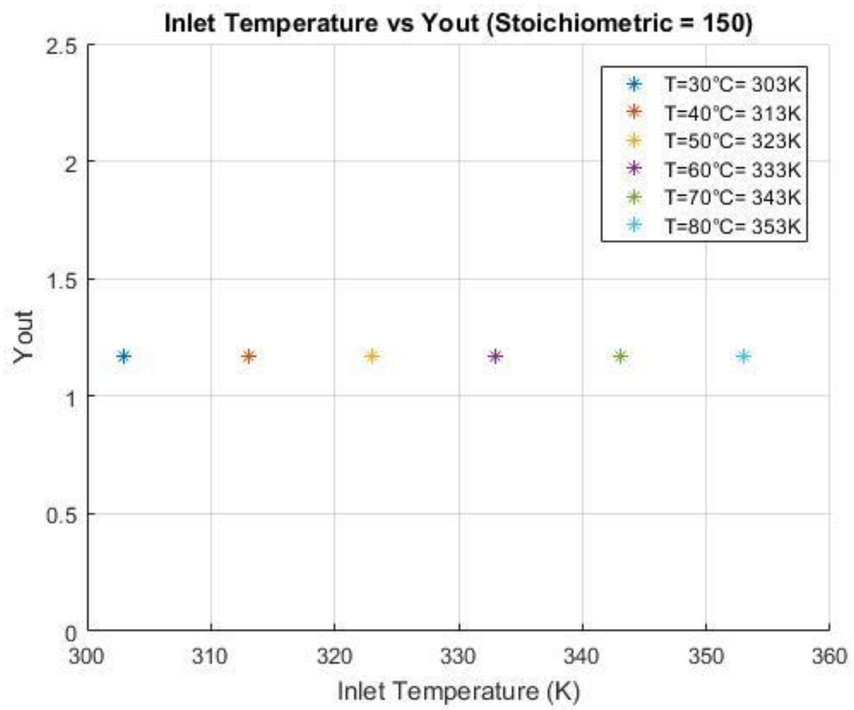

(d)

Figure 5.5: (a) Time vs Difference in Outlet Temperature, (b) Source vs Inlet Temperature,

(c) X_in vs Inlet Temperature, (d) Y_out vs Inlet Temperature

From the figure 5.5.(a), it is observed that the outlet temperature difference is low as the inlet temperature increases. When analysing the equation, from figure 5.5.(b), it is observed that the source value decreases as the inlet temperature increases. In figure 5.5.(c & d), it is observed that the values remain same for varying inlet temperature. So the only varying parameter is the Source. Source depends on voltage and from overpotential curve, figure 3.3, it can be seen that the overpotential value decreases with increase in inlet temperature, i.e. the losses will be less as the temperature increases. It can be explained as, for 30^{o}c the loss will be higher than 80^{o}c. So as the temperature increases the difference in outlet temperature decreases.

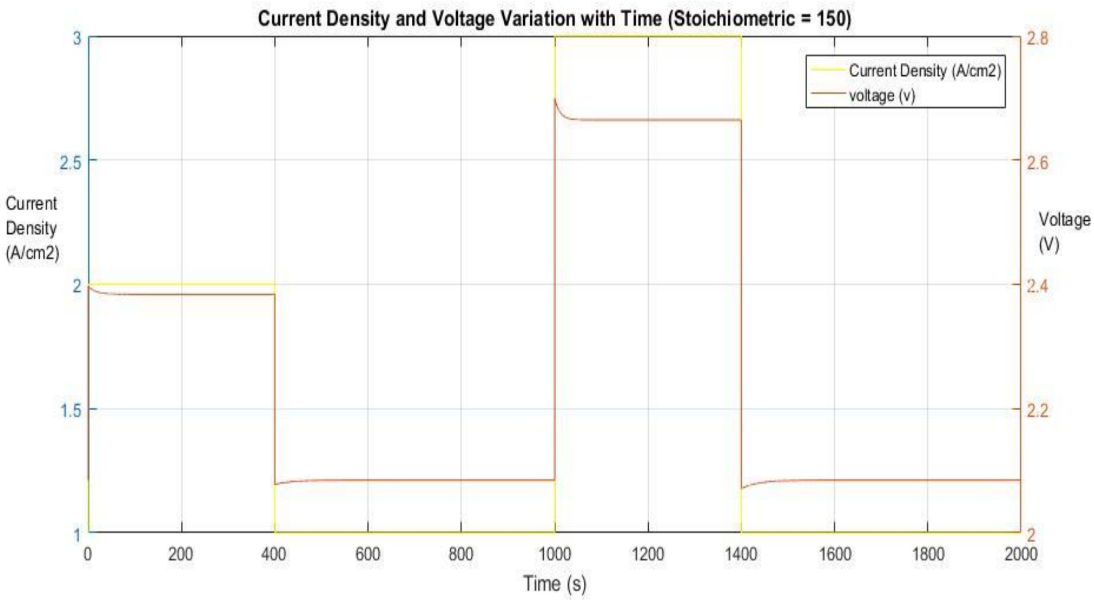

Figure 5.6: Current Density and Voltage with Time

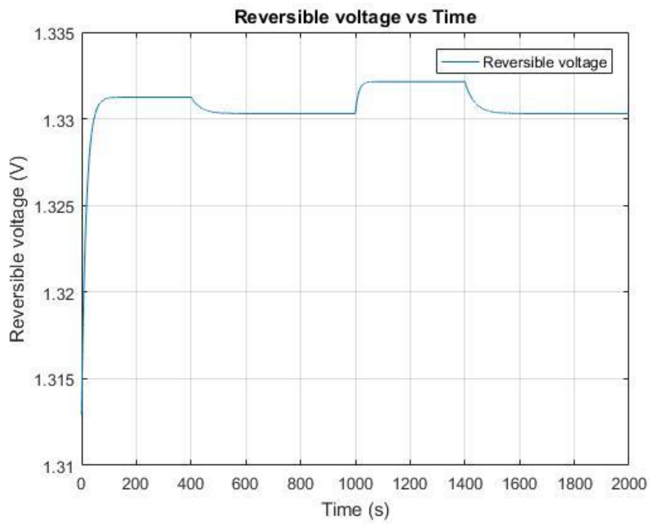

(a)

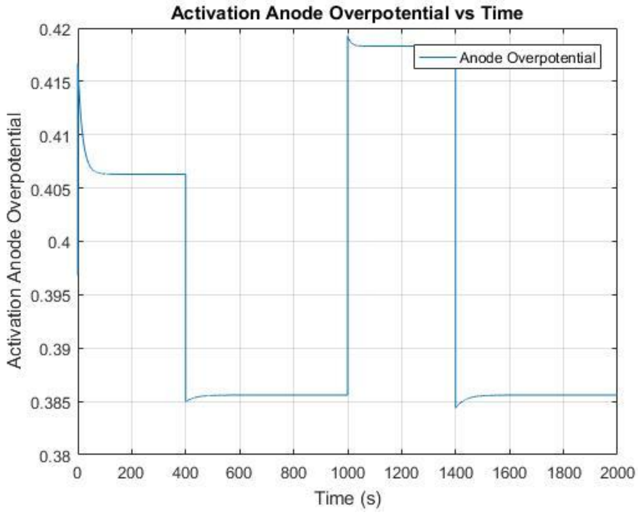
Activation Anode Overpotential vs Time
Anode Overpotential
Activation Anode Overpotential
Time (s)
0.42
0.415
0.41
0.405
0.4
0.395
0.39
0.385
0.38
0
200
400
600
800
1000
1200
1400
1600
1800
2000

(b)

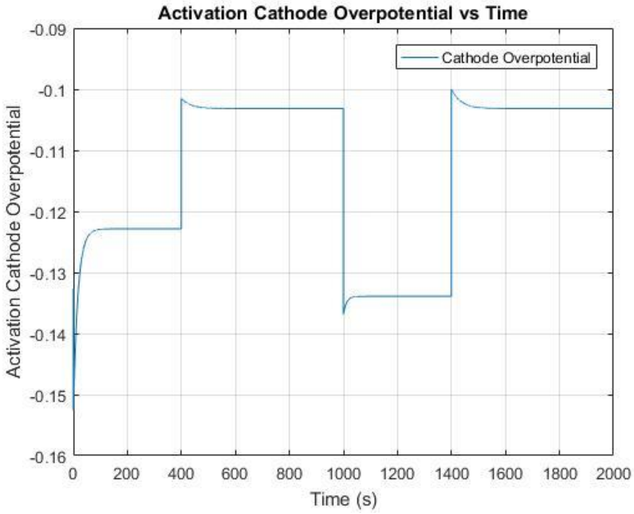
Activation Cathode Overpotential vs Time
Cathode Overpotential
Activation Cathode Overpotential
Time (s)
-0.09
-0.1
-0.11
-0.12
-0.13
-0.14
-0.15
-0.16
0
200
400
600
800
1000
1200
1400
1600
1800
2000

(c)

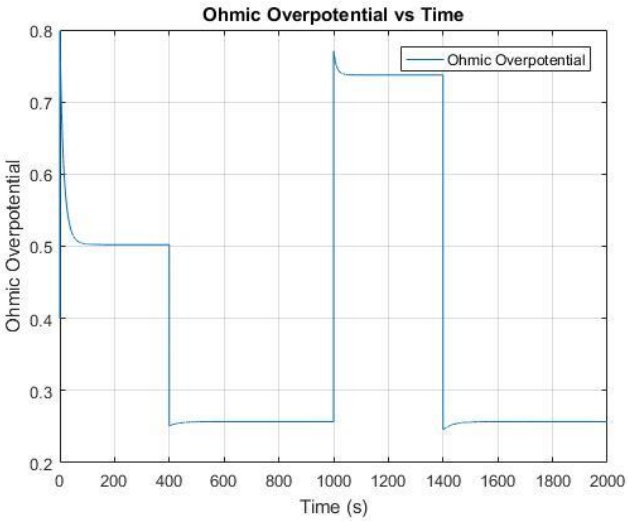
Ohmic Overpotential vs Time
Ohmic Overpotential
Ohmic Overpotential
Time (s)
0.8
0.7
0.6
0.5
0.4
0.3
0.2
0
200
400
600
800
1000
1200
1400
1600
1800
2000

(d)

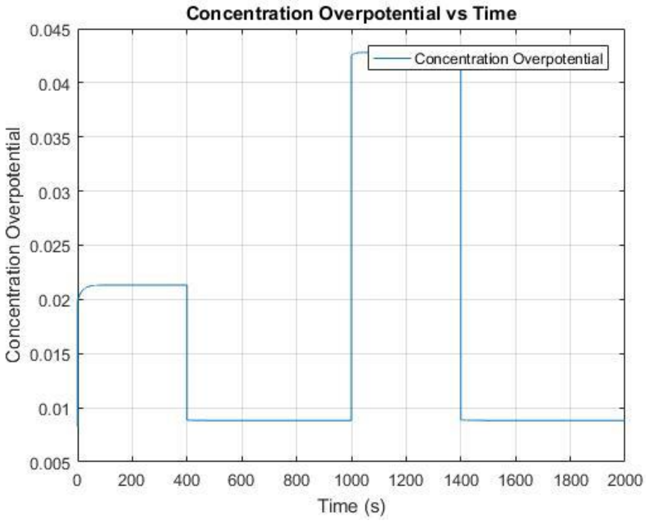

(e)

Figure 5.7: (a) Reversible Voltage (b) Activation Anode Overpotetential (c) Activation Cathode Overpotetential (d) Ohmic Overpotetential (e) Concentration Overpotetential

From figure 5.6, it is inferred that the voltage changes corresponding to the current. But it is noticed that there is a step up or down in voltage where the current changes. Here, the voltage is function of reversible voltage and overpotentials and as seen from figure 5.7, there is shoot up or shoot down in anode, cathode and ohmic overpotentials at the points where the current changes (figure 5.7: b, c & d), i.e, there is much loss happing at these regions. Hence the voltage varies correspondingly.

6. CONCLUSION

A simple dynamic model of a PEM electrolyser, including electrochemical, mass flow and thermal ancillaries has been proposed. The simulation has been done and the plots are studied. For the electrochemical submodel, the fitting parameters were ascribed to physical variables in order to compare with the literature. And the validation was carried out using the data of the literatures. In this study, mathematical model of the dynamic PEM electrolyser was developed. The current verses time, outlet temperature verses time, voltage verses time graphs are plotted at different inlet temperature conditions and stoichiometric. A study of the plots obtained was also done.

This model can be improved by embedding more physics and mathematical expressions and other mass transfer phenomena.

7. FUTURE WORK

Along with embedding more physics and mathematical expressions, this work can be extended by introducing a storage system and a network to distribute hydrogen. Before setting up a hydrogen storage, a study should be done to know the time constant for the mass flow of hydrogen and different parameters that contribute it. The model can also be modified for the pressure variation. If the mass flow rate and pressure varies there should be a compressor or some system to maintain the pressure and to store the hydrogen in the storage tank.

According to me and the literature referred, these are some points that can help to continue the work:

The time lag in the outlet of electrolyser can be occurred due to the losses happen when it flow through the pipe. As we know there are chances of deformation in the pipe that can resist the mass flow.

There are chances of hydrogen storing inside the electrolyser, so there will be two phase inside the electrolyser, liquid and gas. Hence a multiphase flow has to be considered. And also the amount of hydrogen that can be stored inside the electrolyser has to be calculated [33, 34].

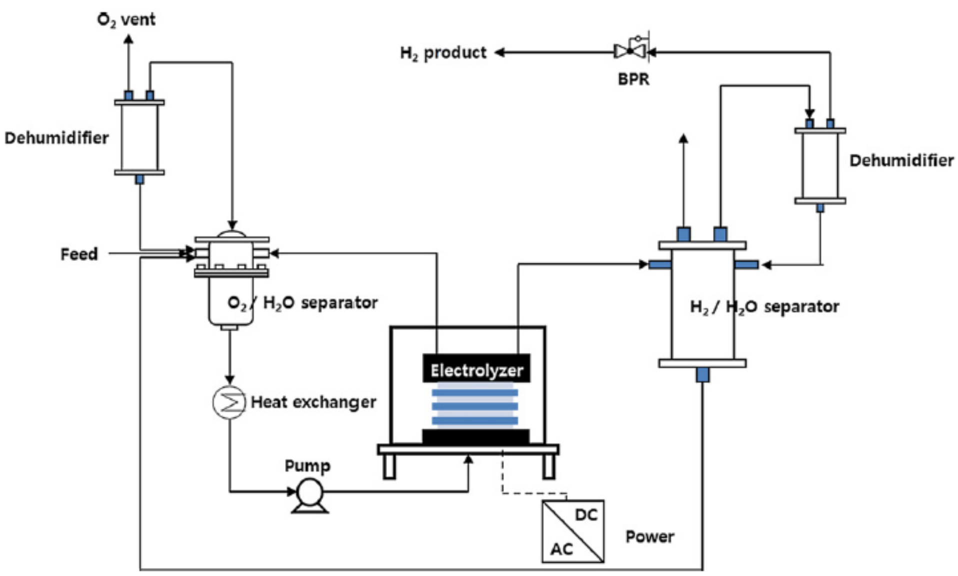

Figure 7.1: High-Pressure Electrolyser System [32]

From the figure 7.1, it is observed that, to get the hydrogen gas from electrolysis there should be some other apparatus attached like separator and dehumidifier. So an efficient apparatus should be selected to avoid the losses.

There is a need of compressor to compress the hydrogen gas before storing into the tank. Hence a control system have to be introduced for the efficient working of the compressor.

8. REFERENCES

1. **G Aragón-González, A León-Galicia, R González-Huerta, J M Rivera Camacho and M Uribe-Salaza.** Hydrogen production by a PEM electrolyser, VII International Congress of Engineering Physics, Journal of Physics: Conference Series **582** (2015) 012054.

2. **F.Z.Aouali, M.Becherif, A.Tabanjat, M.Emziane, K.Mohammedi , S.Krehid, A.Khellaf.** Modelling and experimental analysis of a PEM electrolyser powered by a solar photovoltaic panel, The International Conference on Sustainability in Energy and Buildings, SEB-14, Energy Procedia 62 (2014) 714 – 722.

3. **Meng Ni, Michael K.H. Leung, Dennis Y.C. Leung.** Electrochemistry Modeling of Proton Exchange Membrane (PEM) Water Electrolysis for Hydrogen Production, WHEC 16 / 13-16 June 2006 – Lyon France.

4. **R. Garcı´a-Valverde, N. Espinosa, A. Urbina.** Simple PEM water electrolyser model and experimental Validation, International Journal of Hydrogen Energy 37 (2012) 1927 – 938.

5. **Tevfik Yigit, Omer Faruk Selamet,** Mathematical modeling and dynamic Simulink simulation of high-pressure PEM electrolyzer system, International Journal of Hydrogen Energy 41(2016) 13901-13914.

6. **Choi P, Bessarabovb DG, Dattaa R.** A simple model for solid polymer electrolyte (SPE) water electrolysis. Solid State Ionics 2004; 175: 535-9.

7. **Gorgun H.** Dynamic modelling of a proton exchange membrane (PEM) electrolyzer. Int J Hydrogen Energy 2006; 31: 29e38.

8. **Biaku C, Dale N, Mann M, Salehfar H, Peters A, Han T**. A semiempirical study of the temperature dependence of the anode charge transfer coefficient of a 6 kW PEM electrolyzer. Int J Hydrogen Energy 2008; 33(16):4247e54.

9. **Harrison KW, Hernandez-Pacheco E, Mann M, Salehfar H.** Semiempirical model for determining PEM electrolyzer stack. J Fuel Cell Sci Tech 2006; 3: 220-3.
10. **Dale N, Mann M, Salehfar H.** Semiempirical model based on thermodynamic principles for determining 6 kW proton exchange membrane electrolyzer stack characteristics. J Power Sources 2008; 185(2):1348e53.

11. **Marangio F, Santarelli M, Cali M.** Theoretical model and experimental analysis of a high pressure PEM water electrolyser for hydrogen production. Int J Hydrogen Energy 2009; 34: 1143-58.

12. **Santarelli M, Medina P, Cali M.** Fitting regression model and experimental validation for a high-pressure PEM electrolyzer. Int J Hydrogen Energy 2009; 34: 2519-30.

13. **Lebbal ME, Lecoeuche S.** Identification and monitoring of a PEM electrolyser based on dynamical modelling. Int J Hydrogen Energy 2009; 34(14):5992e9.

14. **Dale NV, Mann MD, Salehfar H.** Semiempirical model based on thermodynamic principles for determining 6kW proton exchange membrane electrolyzer stack characteristics. J Power Sources Dec. 2008; 185(2):1348e53.

15. **Yalcinoz T, Alam MS.** Dynamic modeling and simulation of air-breathing proton exchange membrane fuel cell. J Power Sources 2008; 182: 168-74.

16. **Gorgun H.** Dynamic modeling of a proton exchange membrane (PEM) electrolyzer. Int J Hydrogen Energy 2006; 31: 29-38.

17. **Dale NV, Mann MD, Salehfar H.** Semiempirical model based on thermodynamic principles for determining 6 kW proton exchange membrane electrolyzer stack characterstics. Journal of Power Sources 2008; 185: 1348-53.

18. **Biaku CY, Dale NV, Mann MD, Salehfar H, Peters AJ, Han TA.** Semiempirical study of the temperature dependence of the anode charge transfer coefficient of a 6 kW PEM electrolyzer. Int J Hydrogen Energy 2008; 33: 4247-54.

19. **Santarelli M, Medina P, Cali M.** Fitting regression model and experimental validation for a high pressure PEM electrolyzer. Int J Hydrogen Energy 2009; 34: 2519-30.

20. **Marangio F, Santarelli M, Cali M.** Theoretical model and experimental analysis of a high pressure PEM water electrolyzer for hydrogen production. Int J Hydrogen Energy 2009; 34: 1143-58.

21. **A. Awasthi, Keith Scott, S. Basu.** Dynamic modeling and simulation of a proton exchange membrane electrolyzer for hydrogen production, International Journal of Hydrogen Energy 36 (2011) 14779-14786.

22. **Url-1.** https://energy.gov/eere/fuelcells/hydrogen-production-electrolysis.

23. **C.A. Martinson, G. van Schoor, K.R. Uren , D. Bessarabov.** Characterisation of a PEM electrolyser using the current interrupt method, International Journal of Hydrogen Energy, Volume 39, Issue 36, 12 December 2014, Pages 20865–20878.

24. **Bhanu kiran.A, Y.V.Ramana murty.** Mathematical Modelling and Simulation Analysis of Alkaline Water Electrolyser for Stationary Electrolyte in Atmospheric Pressure, International Journal of Mechanical Engineering and Computer, Applications, Vol 3, Issue 5, Sept – Oct 2015, ISSN 2320-6349.

25. **Julia Mainka.** Local impedance in H2/air Proton Exchange Membrane Fuel Cells (PEMFC) Theoretical and experimental investigations, Doctor Thesis, Laboratoire d'Energétique et de Mécanique Théorique et Appliquée – LEMTA UMR 7563 CNRS Université de Lorraine 54500 Vandoeuvre lès Nancy, 04 July 2011.

26. **Url-2.** https://en.wikipedia.org/wiki/Polymer_electrolyte_membrane_electrolysis.

27. **Bard. Allen J, Faulkner. Larry R** (2001). Electrochemical Methods: Fundamentals and applications. Wiley. ISBN 978-0-471-04372-0.

28. **B.Sunden, M.Faghri.** Transport Phenomena in Fuel Cells, Developments in Heat Transfer, Vol.19, 2005, WIT Press, Southampton, Boston.

29. **Ryan O'hayre, Suk-Won Cha, Whitney Colella, Fritz.B.Prinz.** Fuel Cell Fundamentals, second edition, John Wiley & Sons, Inc, New York.

30. **Url-3.** https://en.wikipedia.org/wiki/limiting_current.

31. **Url-4.** www.engr.uconn.edu. Electrochemistry lectures.

32. **Huiyong Kim, Mikyoung Park, Kwang Soon Lee.** One-dimensional dynamic modeling of a high-pressure water electrolysis system for hydrogen production, International Journal of Hydrogen Energy 38 (2013) 2596 – 2609.

33. **Bo Han, Jingke Mo, Zhenye Kang, Feng-Yuan Zhang.** Effects of membrane electrode assembly properties on two-phase transport and performance in proton exchange membrane electrolyzer cells. Electrochimica Acta 188 (2016) 317 - 326.

34. **I.Dedigama, P. Angeli, K.Ayers, J.B.Robinson, P.R. Shearing, D.Tsaoulidis, D.J.L.Brett.** In situ diagnostic techniques for characterisation of polymer electrolyte membrane water electrolysers – Flow visualisation and electrochemical impedance spectroscopy. International Journal of Hydrogen Energy 39 (2014) 4468 – 4482.

9. APPENDICES

9.1. Polarization Curves

```
clear all
clc
close all

il = 4;
R = 8.314;
F = 96485;
Alpha = 0.5;
n = 2;
Eexc = 53990.065;
sigma_ref = 0.020;
Epro = 18912.42;
delta = 7*2.54*10^-3;


I = 0:0.001:4;
for i = 1:length(I)
    t=0;
    for T = 303:10:353
       t=t+1;

% Anode
ia = (10^-7)*(exp(-(Eexc/R)*((1/T)-(1/298))));
Eta_Anode(i,t) = ((R*T)/(Alpha*n*F))*(log(I(i)/ia));

% Cathode
ic = (10^-3)*(exp(-(Eexc/R)*((1/T)-(1/353))));
Eta_Cathode(i,t) = -((R*T)/(Alpha*n*F))*(log(I(i)/ic));

%Ohmic
sigma(i,T) = sigma_ref*(exp(-(Epro/R)*((1/T)-(1/298))));
Rohm = delta/sigma(i,T);
Eta_Ohmic(i,t) = I(i)*Rohm;

%Concentration
Eta_Conc(i,t) = ((R*T)/(Alpha*n*F))*(log(il/(il-I(i))));

%Voltage
H_h2(i,T)=0+(28.84*(T-298));
H_o2(i,T)=0+(28.91*(T-298));
H_h2o(i,T)=-285830+(75.37*(T-298));
H(i,T)=H_h2(i,T)+(0.5*H_o2(i,T))-H_h2o(i,T);

S_h2(i,T)=130.68+(28.84*(log(T/298)));
S_o2(i,T)=205+(28.91*(log(T/298)));
```

```
S_h2o(i,T)=69.95+(75.37*(log(T/298)));
S(i,T)=S_h2(i,T)+(0.5*S_o2(i,T))-S_h2o(i,T);

G(i,T)=H(i,T)-(T*S(i,T));

E(i,T)=(G(i,T)/(2*F));
ET(i,t) = 1.5184-(1.5421*10^-3*T)+(9.523*10^-5*T*log(T))+(9.84*10^-8*T^2);
EP(i,t)= 1.23+(((R*T)/(n*F))*(log(0.5*0.5^0.5)));
VT(i,t) = ET(i,t) + Eta_Anode(i,t) - Eta_Cathode(i,t) + Eta_Ohmic(i,t) +
Eta_Conc(i,t);
VP(i,t) = EP(i,t) + Eta_Anode(i,t) - Eta_Cathode(i,t) + Eta_Ohmic(i,t) +
Eta_Conc(i,t);
 V(i,t) = E(i,t) + Eta_Anode(i,t) - Eta_Cathode(i,t) + Eta_Ohmic(i,t) + Eta_Conc(i,t);
% disp (['At i = ',num2str(I(i)),' A/cm2',' & T = ',num2str(T),'K',', v = ',
num2str(VT(i,t)),' V']);
% disp (['At i = ',num2str(I(i)),' A/cm2',' & T = ',num2str(T),'K',', v = ',
num2str(VP(i,t)),' V']);

%Mass Flow Rate
A(i) = I(i)* 50;
M_H2(i) = (A(i)*0.99)/(2*F);
M_O2(i) = (A(i)*0.99)/(4*F);
M_H2O(i) = (A(i)*0.99)/(2*F);
disp (['At Current = ',num2str(I(i)),'A',', Mass Flow Rate of H2 = ',
num2str(M_H2(i)),' mol/s',', Mass Flow Rate of O2 = ', num2str(M_O2(i)),' mol/s',',
Mass Flow Rate of H2O = ', num2str(M_H2O(i)),' mol/s']);

   end
end

subplot(3,1,1);
plot (I,V(:,1),I,V(:,2),I,V(:,3),I,V(:,4),I,V(:,5),I,V(:,6))
legend('T=30','T=40','T=50','T=60','T=70','T=80')
xlabel('Current Density (A/cm2)');
ylabel('Cell Voltage (Volt)');
title('I-V Curve (General Equation of E reversible)');

subplot(3,1,2);
plot (I,VP(:,1),I,VP(:,2),I,VP(:,3),I,VP(:,4),I,VP(:,5),I,VP(:,6))
legend('T=30','T=40','T=50','T=60','T=70','T=80')
xlabel('Current Density (A/cm2)');
ylabel('Cell Voltage (Volt)');
title('I-V Curve (Pressure & Temperature variation)');

subplot(3,1,3);
plot (I,VT(:,1),I,VT(:,2),I,VT(:,3),I,VT(:,4),I,VT(:,5),I,VT(:,6))
legend('T=30','T=40','T=50','T=60','T=70','T=80')
xlabel('Current Density (A/cm2)');
ylabel('Cell Voltage (Volt)');
title('I-V Curve (Temperature variation)');
```

```
figure(2);
plot(I,M_H2(:),I,M_H2(:),I,M_H2(:),I,M_H2(:),I,M_H2(:),I,M_H2(:))
xlabel('Current (A/cm2)');
ylabel('Molar Flow Rate (mol/s)');
title('Current vs Molar Flow Rate of H2');

figure(3);
plot(I,Eta_Anode(:,1),I,Eta_Anode(:,2),I,Eta_Anode(:,3),I,Eta_Anode(:,4),I,Eta_Ano
de(:,5),I,Eta_Anode(:,6),I,Eta_Cathode(:,1),I,Eta_Cathode(:,2),I,Eta_Cathode(:,3),I,E
ta_Cathode(:,4),I,Eta_Cathode(:,5),I,Eta_Cathode(:,6),I,Eta_Ohmic(:,1),I,Eta_Ohmic
(:,2),I,Eta_Ohmic(:,3),I,Eta_Ohmic(:,4),I,Eta_Ohmic(:,5),I,Eta_Ohmic(:,6),I,Eta_Co
nc(:,1),I,Eta_Conc(:,2),I,Eta_Conc(:,3),I,Eta_Conc(:,4),I,Eta_Conc(:,5),I,Eta_Conc(:,
6))
legend('T=30','T=40','T=50','T=60','T=70','T=80')
xlabel('Current Density (A/cm2)');
ylabel('Overpotential (Volt)');
title('Different Overpotential');

figure(4);
subplot(2,2,1);
plot(I,Eta_Anode(:,1),I,Eta_Anode(:,2),I,Eta_Anode(:,3),I,Eta_Anode(:,4),I,Eta_Ano
de(:,5),I,Eta_Anode(:,6))
xlabel('Current Density (A/cm2)');
ylabel('Overpotential (Volt)');
title('Activation Anode Overpotential');

subplot(2,2,2);
plot(I,Eta_Cathode(:,1),I,Eta_Cathode(:,2),I,Eta_Cathode(:,3),I,Eta_Cathode(:,4),I,Et
a_Cathode(:,5),I,Eta_Cathode(:,6))
xlabel('Current Density (A/cm2)');
ylabel('Overpotential (Volt)');
title('Activation Cathode Overpotential');

subplot(2,2,3);
plot(I,Eta_Ohmic(:,1),I,Eta_Ohmic(:,2),I,Eta_Ohmic(:,3),I,Eta_Ohmic(:,4),I,Eta_Oh
mic(:,5),I,Eta_Ohmic(:,6))
xlabel('Current Density (A/cm2)');
ylabel('Overpotential (Volt)');
title('Ohmic Overpotential');
subplot(2,2,4);

plot(I,Eta_Conc(:,1),I,Eta_Conc(:,2),I,Eta_Conc(:,3),I,Eta_Conc(:,4),I,Eta_Conc(:,5),
I,Eta_Conc(:,6))
xlabel('Current Density (A/cm2)');
ylabel('Overpotential (Volt)');
title('Concentration Overpotential');
```

9.2. Dynamic Model

```
clear
clc
global Tout_intial
close all
lamdaA = 150;% Stoichiometric
lamdaC = 150;
F = 96485;%Faraday Constant, C/mol
il = 4;% Limiting Current, A/cm^2
i0a = 10^-7;% Current Density at Anode, A/cm^2
i0c = 10^-3;% Current Density at Cathode, A/cm^2
R = 8.314;% Universal Gas Constant, J/mol.K
s = 10;% Surface Area, cm^2
Cp_H2O = 4179;% Specific Heat of Water, J/kg.K
Cp_H2 = 14337;% Specific Heat of Hydrogen, J/kg.K
Cp_O2 = 920.5;% Specific Heat of Oxygen, J/kg.K
Rho_H2O = 1*10^-3;% Density of Water, Kg/cm^3
% v = 2*500*10^-7;% volume, cm^3
v = s*1; % volume, cm^3
Alpha = 0.5;% Charge Transfer coefficient
n = 2;% Stoichiometric Coefficient for Transferred Electrons
Eexc = 53990.065;% Activation Energy for Electrode Reaction, J/mol
sigma_ref = 0.020;% Reference Conductivity of Membrane, S/cm
Epro = 18912.42;% Activation Energy for Proton Transport in Membrane, J/mol
delta = 7*2.54*10^-3;% Thickness of Membrane, cm
T_in = 303:10:353;
IV = 1; % A/cm^2

for j = 1:numel(T_in)
   To(j) = T_in(j);   %inital guess
   Diff = 1;
   Temp = 0;
 while(Diff > 1e-16)
        M_H2Oin_a = ((1+lamdaA)*(IV*s*18*10^-3))/(2*F);
        M_H2Oout_a = ((lamdaA)*(IV*s*18*10^-3))/(2*F);
        M_H2Oin_c = (lamdaC)*(IV*s*18*10^-3)/(2*F);
        M_H2Oout_c = (lamdaC)*(IV*s*18*10^-3)/(2*F);
        M_H2out_c = (IV*s*2*10^-3)/(2*F);
        M_O2out_a = (IV*s*32*10^-3)/(4*F);

        T = (T_in(j)+ To(j))/2;
        % Anode
        ia = (i0a)*(exp(-(Eexc/R)*((1/T)-(1/298))));
        Eta_Anode = ((R*T)/(Alpha*n*F))*(log(IV/ia));
        % Cathode
        ic = (i0c)*(exp(-(Eexc/R)*((1/T)-(1/298))));
        Eta_Cathode = -((R*T)/(Alpha*n*F))*(log(IV/ic));
        %Ohmic
        sigma = sigma_ref*(exp(-(Epro/R)*((1/T)-(1/298))));
        Rohm = delta/sigma;
        Eta_Ohmic = IV*Rohm;
```

```
        %Concentration
        Eta_Conc = ((R*T)/(Alpha*n*F))*(log(il/(il-IV)));
        % Enthalpy
        H_H2 = 0+(28.84*(T-298));
        H_O2 = 0+(28.91*(T-298));
        H_H2O = -285830+(75.37*(T-298));
        delta_H = H_H2+(0.5*H_O2)-H_H2O;
        % voltage
        S_h2 = 130.68+(28.84*(log(T/298)));
        S_o2 = 205+(28.91*(log(T/298)));
        S_h2o = 69.95+(75.37*(log(T/298)));
        S = S_h2+(0.5*S_o2)-S_h2o;
        E = 1.299+((S*(T-298))/(n*F))+(((R*T)/(n*F))*(log(0.5*0.5^0.5)));

        V = E + Eta_Anode - Eta_Cathode + Eta_Ohmic + Eta_Conc;

        X_in = (M_H2Oin_a*Cp_H2O)+(M_H2Oin_c*Cp_H2O);
        Q = (V-(delta_H/(2*F)))*IV*s;
        Y_out =
(M_H2Oout_a*Cp_H2O)+(M_H2Oout_c*Cp_H2O)+(M_H2out_c*Cp_H2)+(M_O2
out_a*Cp_O2);
        Z = Rho_H2O*Cp_H2O*v;
           To(j) = ((X_in*T_in(j))+Q-(Y_out*To(j)))/Z*0.6 + To(j);
      Diff = To(j) - Temp;
      Temp = To(j);
 end
end
Tout_intial = To;
```

9.3. Main Program

```
clear
clc
close all
global Tout_intial
% lamdaA = 150;% Stoichiometric
lamdaC = 150;
F = 96485;%Faraday Constant, C/mol
il = 4;% Limiting Current, A/cm^2
i0a = 10^-7;% Current Density at Anode, A/cm^2
i0c = 10^-3;% Current Density at Cathode, A/cm^2
R = 8.314;% Universal Gas Constant, J/mol.K
s = 10;% Surface Area, cm^2
Cp_H2O = 4179;% Specific Heat of Water, J/kg.K
Cp_H2 = 14337;% Specific Heat of Hydrogen, J/kg.K
Cp_O2 = 920.5;% Specific Heat of Oxygen, J/kg.K
Rho_H2O = 1*10^-3;% Density of Water, Kg/cm^3
% v = 2*500*10^-7;% volume, cm^3
v = s*1; % volume, cm^3
Alpha = 0.5;% Charge Transfer coefficient
```

```
n = 2;% Stoichiometric Coefficient for Transferred Electrons
Eexc = 53990.065;% Activation Energy for Electrode Reaction, J/mol
sigma_ref = 0.020;% Reference Conductivity of Membrane, S/cm
Epro = 18912.42;% Activation Energy for Proton Transport in Membrane, J/mol
delta = 7*2.54*10^-3;% Thickness of Membrane, cm
T_in = 303:10:353;

for c = 1:numel(lamdaC)
    co=hsv(length(T_in));
for j = 1:numel(T_in)
    tf=2000;
    t1=0; %if t>t1 I=2A/cm2;
    t2=400; %if t>t2 I=1A/cm2;
    t3=1000;
    t4=1400;
    tdf=tf/20000;
    time=0:tdf:tf;
    I0=2; %A/cm^2
    I1=3;
    IV=ones(1,length(time));

    for t = 1:numel(time)
        if t1 <time(t) && time(t) <t2
            IV(t) = I0;
        end
         if t3 <time(t) && time(t) <t4
            IV(t) = I1;
        end
        M_H2Oin_a = ((1+lamdaC(c))*(IV(t)*s*18*10^-3))/(2*F);
        M_H2Oout_a = ((lamdaC(c))*(IV(t)*s*18*10^-3))/(2*F);
        M_H2Oin_c = (lamdaC(c))*(IV(t)*s*18*10^-3)/(2*F);
        M_H2Oout_c = (lamdaC(c))*(IV(t)*s*18*10^-3)/(2*F);
        M_H2out_c = (IV(t)*s*2*10^-3)/(2*F);
        M_O2out_a = (IV(t)*s*32*10^-3)/(4*F);

        if t > 1
            T = (T_in(j)+ To(t-1))/2;
        % Anode
        ia = (i0a)*(exp(-(Eexc/R)*((1/T)-(1/298))));
        Eta_Anode = ((R*T)/(Alpha*n*F))*(log(IV(t)/ia));
        % Cathode
        ic = (i0c)*(exp(-(Eexc/R)*((1/T)-(1/298))));
        Eta_Cathode = -((R*T)/(Alpha*n*F))*(log(IV(t)/ic));
        %Ohmic
        sigma = sigma_ref*(exp(-(Epro/R)*((1/T)-(1/298))));
        Rohm = delta/sigma;
        Eta_Ohmic = IV(t)*Rohm;
        %Concentration
        Eta_Conc = ((R*T)/(Alpha*n*F))*(log(il/(il-IV(t))));
        % Enthalpy
```

```
        H_H2 = 0+(28.84*(T-298));
        H_O2 = 0+(28.91*(T-298));
        H_H2O = -285830+(75.37*(T-298));
        delta_H = H_H2+(0.5*H_O2)-H_H2O;
        % voltage
        S_h2 = 130.68+(28.84*(log(T/298)));
        S_o2 = 205+(28.91*(log(T/298)));
        S_h2o = 69.95+(75.37*(log(T/298)));
        S = S_h2+(0.5*S_o2)-S_h2o;
        E = 1.299+((S*(T-298))/(n*F))+(((R*T)/(n*F))*(log(0.5*0.5^0.5)));

        V(t) = E + Eta_Anode - Eta_Cathode + Eta_Ohmic + Eta_Conc;

        X_in = (M_H2Oin_a*Cp_H2O)+(M_H2Oin_c*Cp_H2O);
        Q = (V(t)-(delta_H/(2*F)))*IV(t)*s;
        Y_out =
(M_H2Oout_a*Cp_H2O)+(M_H2Oout_c*Cp_H2O)+(M_H2out_c*Cp_H2)+(M_O2
out_a*Cp_O2);
        Z = Rho_H2O*Cp_H2O*v;

        To(t) = ((X_in*T_in(j))+Q-(Y_out*To(t-1)))/Z*tdf + To(t-1);
        P(t) = V(t)*IV(t)*s; % Power
        else
            T = (T_in(j)+ Tout_intial(j))/2;
            % Anode
        ia = (i0a)*(exp(-(Eexc/R)*((1/T)-(1/298))));
        Eta_Anode = ((R*T)/(Alpha*n*F))*(log(IV(t)/ia));
        % Cathode
        ic = (i0c)*(exp(-(Eexc/R)*((1/T)-(1/298))));
        Eta_Cathode = -((R*T)/(Alpha*n*F))*(log(IV(t)/ic));
        %Ohmic
        sigma = sigma_ref*(exp(-(Epro/R)*((1/T)-(1/298))));
        Rohm = delta/sigma;
        Eta_Ohmic = IV(t)*Rohm;
        %Concentration
        Eta_Conc = ((R*T)/(Alpha*n*F))*(log(il/(il-IV(t))));
        % Enthalpy
        H_H2 = 0+(28.84*(T-298));
        H_O2 = 0+(28.91*(T-298));
        H_H2O = -285830+(75.37*(T-298));
        delta_H = H_H2+(0.5*H_O2)-H_H2O;
        % voltage
        S_h2 = 130.68+(28.84*(log(T/298)));
        S_o2 = 205+(28.91*(log(T/298)));
        S_h2o = 69.95+(75.37*(log(T/298)));
        S = S_h2+(0.5*S_o2)-S_h2o;
        E = 1.299+((S*(T-298))/(n*F))+(((R*T)/(n*F))*(log(0.5*0.5^0.5)));

        V(t) = E + Eta_Anode - Eta_Cathode + Eta_Ohmic + Eta_Conc;
```

```
        X_in = (M_H2Oin_a*Cp_H2O)+(M_H2Oin_c*Cp_H2O);
        Q = (V(t)-(delta_H/(2*F)))*IV(t)*s;
        Y_out =
(M_H2Oout_a*Cp_H2O)+(M_H2Oout_c*Cp_H2O)+(M_H2out_c*Cp_H2)+(M_O2
out_a*Cp_O2);
        Z = Rho_H2O*Cp_H2O*v;
        To(t)= Tout_intial(j);
        P(t) = V(t)*IV(t)*s; % Power
        end
    end


    Diff =  To-To(1);
    figure(1)
    set(gcf,'color',[1 1 1])
    plot(time,To,'Color',co(j,:));
    hold on;
    grid on
    legend('T=30°C= 303K','T=40°C= 313K','T=50°C= 323K','T=60°C=
333K','T=70°C= 343K','T=80°C= 353K')
    xlabel('Time (s)');
    ylabel('Outlet Temperature (K)');
    title('Time vs Outlet Temperature Curve');
    figure(2)
    set(gcf,'color',[1 1 1])
    plot(time,Diff,'Color',co(j,:));
    hold on;
    grid on
    legend('T=30°C= 303K','T=40°C= 313K','T=50°C= 323K','T=60°C=
333K','T=70°C= 343K','T=80°C= 353K')
    xlabel('Time (s)');
    ylabel('Temperature variation: T(t)-T(t=0)');
    title('Time vs Difference of Outlet Temperature (Stoichiometric = 150)');
    figure(20)
    set(gcf,'color',[1 1 1])
    plot(time,Diff./max(Diff),'Color',co(j,:));
    hold on;
    grid on
    legend('T=30°C= 303K','T=40°C= 313K','T=50°C= 323K','T=60°C=
333K','T=70°C= 343K','T=80°C= 353K')
    xlabel('Time (s)');
    ylabel('Temperature variation: T(t)-T(t=0)');
    title('Time vs Difference of Outlet Temperature (Stoichiometric = 150)');
    figure(3)
    set(gcf,'color',[1 1 1])
    hold on;
    plot(T_in(j),X_in,'*');
    grid on
    legend('T=30°C= 303K','T=40°C= 313K','T=50°C= 323K','T=60°C=
333K','T=70°C= 343K','T=80°C= 353K')
```

```
    xlabel('Inlet Temperature (K)');
    ylabel('Xin');
    title('Inlet Temperature vs X in (Stoichiometric = 150)');
    figure(4)
    set(gcf,'color',[1 1 1])
    hold on;
    plot(T_in(j),Q,'*');
    grid on
    legend('T=30°C= 303K','T=40°C= 313K','T=50°C= 323K','T=60°C=
333K','T=70°C= 343K','T=80°C= 353K')
    xlabel('Inlet Temperature (K)');
    ylabel('Source');
    title('Inlet Temperature vs Q (Stoichiometric = 150)');
    figure(5)
    set(gcf,'color',[1 1 1])
    hold on;
    plot(T_in(j),Y_out,'*');
    grid on
    legend('T=30°C= 303K','T=40°C= 313K','T=50°C= 323K','T=60°C=
333K','T=70°C= 343K','T=80°C= 353K')
    xlabel('Inlet Temperature (K)');
    ylabel('Yout');
    title('Inlet Temperature vs Yout (Stoichiometric = 150)');

end
end
figure(10)
set(gcf,'color',[1 1 1])
plotyy(time,IV,time,To);
grid on
legend('Current Density (A/cm2)','Temperature (K)');
xlabel('Time (s)');
title('Current Density and Outlet Temperature with Time (Stoichiometric = 150)');
    figure(11)
    set(gcf,'color',[1 1 1])
    plotyy(time,IV,time,V);
    hold on;
    grid on
    legend('Current Density (A/cm2)','voltage (v)');
    xlabel('Time (s)');
    title('Current Density and Voltage Variation with Time (Stoichiometric = 150)');
    D_Vol = V-V(1);

    figure(110)
    set(gcf,'color',[1 1 1])
    plot(time,D_Vol)
    grid on
    legend('voltage (v)');
    xlabel('Time (s)');
```

```
figure(12)
    set(gcf,'color',[1 1 1])
    plotyy(time,IV,time,P);
    hold on;
    grid on
    legend('Current Density (A/cm2)','Power');
    xlabel('Time (s)');
    title('Current Density and Power Variation with Time (Stoichiometric = 150)');
```